Determination of interfacial roughness correlation in W/C multilayer films: Comparison using soft and hard x-ray diffraction

D. E. Savage, Y.-H. Phang, J. J. Rownd, J. F. MacKay,[a] and M. G. Lagally
University of Wisconsin, Materials Science Program, 1500 Johnson Dr., Madison, Wisconsin 53706

(Received 27 May 1993; accepted for publication 29 July 1993)

Interfacial roughness correlation in W/C multilayer films with periods of 23, 30, and 37 Å is examined with x-ray diffraction using λ in the 10–13 Å range and $\lambda = 1.54$ Å. Transverse scans through multilayer Bragg reflections are analyzed to determine the magnitude and lateral correlation length of the component of interfacial roughness that is perfectly correlated through the multilayer stack. The results are independent of wavelength, even though hard x rays sample much more deeply into the film, indicating that interfacial roughness is not changing through these films.

I. INTRODUCTION

Multilayer thin films have become increasingly important for applications in soft x-ray optics. Because x rays interact only weakly with matter, they will penetrate many layers of a sample, scattering only slightly at each interface. However, if a Bragg condition of the multilayer is satisfied, x rays will scatter from each interface in phase, giving rise to an appreciable reflected intensity. This ability makes multilayer films attractive for applications where high reflectivity at near-normal incidence is desirable. Multilayer reflectors have been used successfully in a range of applications, including x-ray lithography,[1] x-ray microscopy,[2–4] and x-ray astronomy.[5,6]

One of the major factors that can limit the performance of multilayer soft x-ray optical components is the presence of interfacial roughness, particularly roughness that is replicated through the multilayer stack. It is well known that interfacial roughness, independent of how it is correlated from layer to layer, will reduce the specular intensity, redistributing it into a diffuse background.[7,8] However, roughness that is replicated through the film will have the additional effect of maximizing the diffusely scattered intensity at the Bragg conditions of the multilayer.[9] Thus correlated roughness will concentrate the diffuse intensity into a halo around the specular beam, limiting contrast in imaging applications.

Direct measurements of the angular distributions of hard x rays ($\lambda < 1.54$ Å) scattered from multilayers to explore the nature of interfacial roughness have recently been made. Systems that have been studied include sputter deposited films of W/C[10,11] and Mo/Si[12] used for soft x-ray optics, sputter deposited metallic multilayers developed for magnetic applications,[13] and single-crystal semiconductor multiple-quantum-well structures grown by molecular beam epitaxy (MBE).[14–18] In all cases, the distribution of the diffuse intensity in the vicinity of the specular reflection was resolved clearly, indicating some component of correlated roughness. A model developed originally to explain results from W/C multilayers suggests that interfacial roughness can be divided into vertically correlated and noncorrelated components.[10] It was used to obtain quantitative estimates for the magnitude of the correlated roughness and its lateral correlation length. The *rms* roughness of the correlated component was found to be significant for all W/C samples (independent of the number of bilayers and the bilayer period), with a magnitude $\sigma_{corr} \sim 1$–2 Å compared with the total roughness, with a magnitude $\sigma_{total} \sim 2.5$–4 Å. The lateral correlation length of the correlated component was determined to be on the order of ~ 50–100 Å. For the other types of sample films, similar values of correlated roughness, but with correlation lengths up to several thousands of angstroms for MBE-grown films have been found.

Further work has extended the model to include the possibility that roughness may be partially correlated from layer to layer.[15,19–21] Detailed measurements of W/C multilayers show that while interfacial roughness in this materials combination is highly correlated, the correlation is not perfect.[22] It can be shown, however, that the assumption of perfect correlation determines a lower limit for the magnitude of correlated roughness and an upper limit for the lateral correlation length.[10]

Recently, it was questioned, on the basis of outer-surface roughness measurements with scanning tunneling microscopy and optical profilometry on Co/C multilayers,[23] whether interfacial roughness can be as well correlated as has been suggested by the $\lambda = 1.54$ Å measurements described above.[10] The magnitude of this roughness, if correlated through the sample, would give unacceptable contrast in Co/C multilayer films used as optical components in a soft x-ray telescope. However, measurements of the moon's shadow edge made during a solar eclipse with $\lambda = 63.5$ Å x rays shows diffraction-limited resolution. These measurements were used to obtain upper limits on the contributions of different spatial frequencies to the rms roughness. For roughness wavelengths in the range of 0.1–1 μm the rms roughness was of the order of 1 Å, while smaller values were obtained for wavelengths beyond 1 μm. The magnitude of the outer-surface roughness was an order of magnitude larger.

It therefore is an important question to consider whether roughness builds up as the number of layers in-

[a]Department of Medical Physics, Medical Science Center, University of Wisconsin, Madison, WI.

 © 1993 American Institute of Physics

Downloaded 27 Aug 2010 to 148.6.178.100. Redistribution subject to AIP license or copyright; see http://jap.aip.org/about/rights_and_permissions

creases. Such a buildup has been observed using cross-sectional transmission electron microscopy (CTEM) in Nb/Si superlattices sputter deposited at high pressure (15 MTorr).[24] The high pressure leads to more off-normal deposition, enhancing shadowing and causing protrusions to grow preferentially. These protrusions are then both copied and enhanced as more layers are deposited. On the other hand, the evidence from CTEM is not conclusive for multilayers grown under optimal conditions. The distinctive roughness buildup is then not observed. In any case, CTEM is not the ideal tool, because roughness with wavelengths on the order of or less than the film cross-section is averaged out as electrons transmit through the sample. X-ray diffraction is sensitive to small as well as large length scales.

While it may be possible to reconcile the performance of a soft-x-ray optical device with a hard-x-ray characterization of morphology, one must establish the limits for which such a characterization is justified. First, for a given incidence angle, longer-wavelength x rays probe a smaller sample volume. If interfacial roughness increases during the deposition process, soft x rays, sensitive preferentially to the upper interfaces, would see a larger rms roughness than would hard x rays. This statement is not strictly correct, as using hard x rays at grazing incidence also produces surface sensitivity. To take advantage of surface sensitivity at grazing incidence requires measurement of the first-order Bragg condition; however, the grazing incidence then does not permit a wide range of angles to be observed in the rocking curve. To circumvent this limitation,[10] measurements are typically made at higher-order Bragg peaks, which occur at less grazing angles, with correspondingly less surface sensitivity, because the path length in the sample changes rapidly with angle.

Second, softer x-rays will not be as sensitive to roughness on the atomic scale, i.e., lateral-scale roughness shorter than their wavelength. Such roughness will appear as a change in layer composition. The specularly reflected intensity will be reduced, but the lost intensity would not be scattered into a diffuse background but instead coupled into the transmitted beam. Third, predictions on how a soft-x-ray optical device will perform based on extrapolations from measurements with $\lambda=1.54$ Å will depend on the accuracy of the model of interfacial structure. Therefore, the most direct approach to characterize a soft-x-ray optical device is to measure its properties at the operating wavelength.

In this work, we compare angular distributions of x-rays scattered from W/C multilayer mirrors using different wavelengths, $\lambda=1.54$ Å and λ in the range from 10 to 13 Å. These experiments are part of an ongoing effort to develop highly reflective soft x-ray mirrors for a multilayer monochromator[25] installed on the Aladdin Synchrotron at the University of Wisconsin-Madison. Measurements of the angular distribution determine unambiguously the contribution of the diffusely scattered intensity in the vicinity of the specular beam for soft x-rays. In addition, comparison of results at different wavelengths lets us evaluate whether using $\lambda=1.54$ Å can predict performance at other wavelengths. We extract the magnitude and lateral correlation length of the vertically correlated roughness in these wavelength ranges.

II. EXPERIMENT

Multilayer samples were deposited in a dc magnetron sputtering system with a base pressure of 3×10^{-7} Torr. Substrates were loaded on a rotary table and passed alternately over C and W sources. The sputtering gas was Ar with a partial pressure during deposition of 1.5 mTorr. Deposition is nominally at room temperature, although substrates may reach 100 °C for some deposition conditions. For the samples discussed here, the C and W layers were chosen to be approximately equal. The Si(100) wafers used for substrates were prepared by rinsing in ethanol.

Results from three samples will be described. Sample 1 has 20 bilayers with a 37 Å period. Sample 2 has 55 bilayers with a 30 Å period. Sample 3 has 70 bilayers with a 23 Å period.

Diffraction measurements using $\lambda=1.54$ Å were performed on a conventional two-circle diffractometer. The angles between source and sample (ω) and between source and detector (2θ) can be varied independently and are stepper motor controlled to an accuracy of 0.002°. The source is a Cu x-ray tube and the detector incorporates a graphite monochromator set to detect Cu $K\alpha$ radiation. The source is defined by slits of 0.03° width in the plane of diffraction while the detector aperture slits are set to subtend an angle of 0.01°. Relative intensities are determined by normalizing to the primary-beam intensity.

Soft-x-ray measurements were performed on a two-circle diffractometer attached to a double-multilayer-mirror monochromator installed on the Aladdin synchrotron. The double-mirror monochromator delivers high flux over the energy range of 100–2000 eV ($\lambda=124$–6 Å). The high flux is achieved by using W/C multilayer mirrors as reflectors at the expense of energy resolution. The relatively large band pass of the monochromator, $\Delta E/E=0.04$, has, however, little effect on the measurements that will be presented. The primary beam is collimated in the plane of diffraction by a 0.5 mm slit 1 m from the second mirror of the monochromator and 7 m from the source radiation and so can be treated as parallel. The detector is a Si photodiode and is collimated in the plane of the diffraction by a 0.5 mm slit located 110 mm from the sample. The incident beam is attenuated by a 7 μm thick Be filter to eliminate low-energy light that would otherwise be transmitted by the monochromator.

In Fig. 1, we illustrate three different ways by which the scattered-intensity distribution is probed. We plot the intensity distribution as a function of the momentum transfer vector S, where $S=K_{out}-K_{in}$ and the K's are wave propagation vectors. The (ω, 2θ) scan, a measure of the specular intensity as a function of incidence angle ω, probes the intensity distribution normal to the surface. The offset (ω,2θ) scan is achieved by rotating the crystal a fixed amount and then making a conventional (ω,2θ) scan. This

Downloaded 27 Aug 2010 to 148.6.178.100. Redistribution subject to AIP license or copyright; see http://jap.aip.org/about/rights_and_permissions

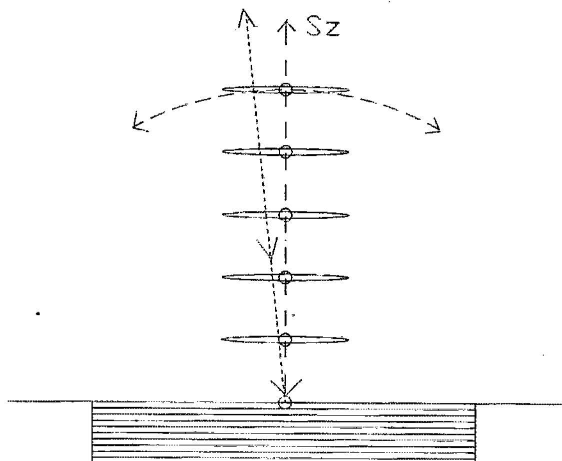

FIG. 1. Schematic view showing how three different experimental scans probe reciprocal space. S_z is defined as lying along the sample normal and has a magnitude $(2\pi/\lambda)[\sin(\omega)+\sin(2\theta-\omega)]$. S_x is parallel to the plane of the surface and has a magnitude $(4\pi/\lambda)[\sin(\theta)\sin(\omega-\theta)$.

measures the diffuse intensity distribution normal to the surface. Finally, the rocking curve probes the intensity distribution parallel to the sample surface.

III. RESULTS

In this section we compare measurements of interfacial roughness at different wavelengths. Figure 2 shows Cu $K\alpha$ $(\omega,2\theta)$ scans for each sample. There is significant intensity out to large angles, indicating that the interfaces in these films are relatively smooth. We extract the film period fitting the peak positions to a modified Bragg's law.[26] Quantitative values for the average interface roughness are obtained by modeling the specular intensity using a Fresnel diffraction calculation,[27] in which σ, the interface roughness, and Γ, the thickness of the W layer relative to the film period, are the fit parameters. By using a single value for σ, we are assuming that interfacial roughness is static, i.e., each interface has the same average roughness. The results of the fits are plotted as solid lines in Fig. 2. Sample 1,

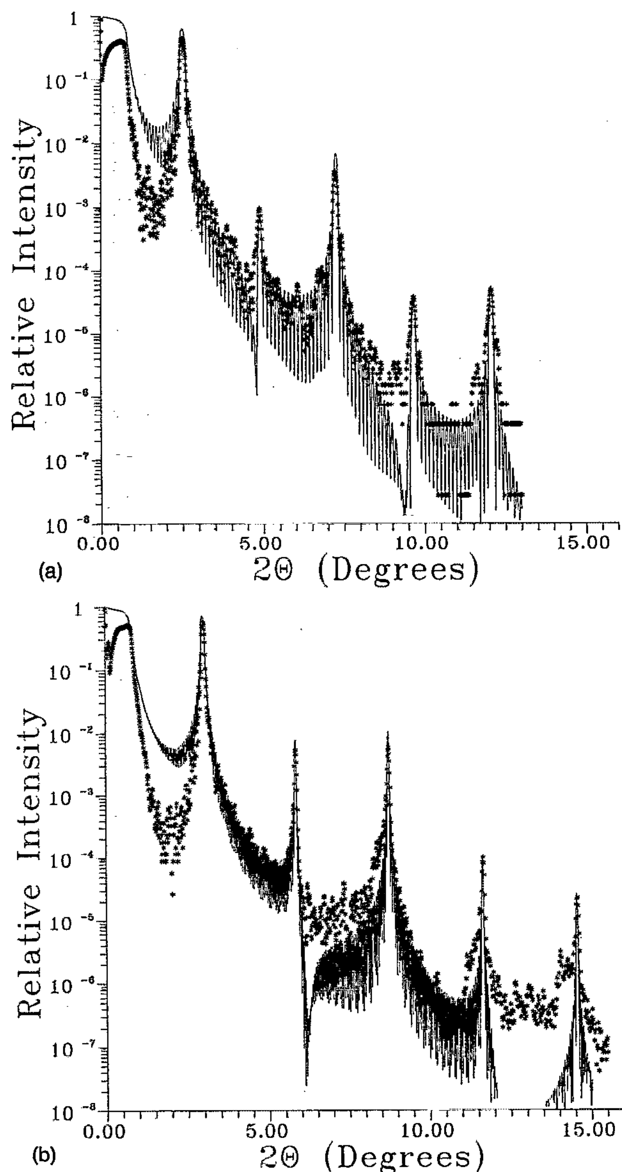

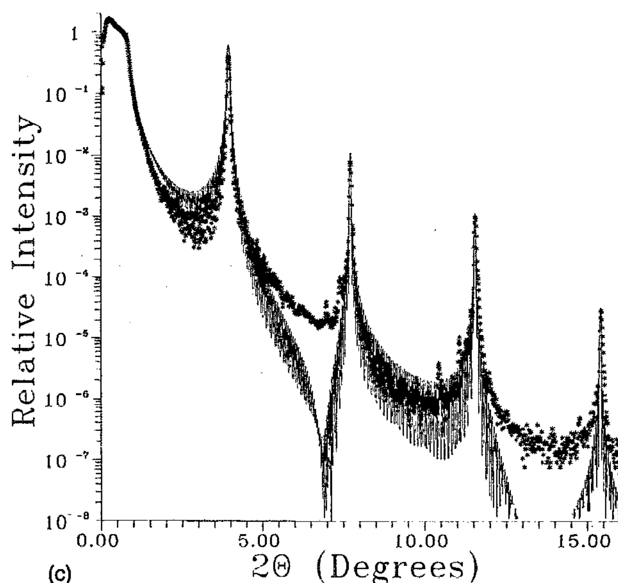

FIG. 2. $(\omega,2\theta)$ scans measuring specular intensity using $\lambda=1.54$ Å radiation. The solid curves are theoretical fits. (a) Sample 1 ($N=20$ $d=36.7$ Å): Fit with an interfacial roughness $\sigma_{total}=2.45$ Å and $\Gamma=0.52$. (b) Sample 2 ($N=55$ $d=30.46$ Å): $\sigma_{total}=2.4$ Å and $\Gamma=0.47$. (c) Sample 3 ($N=70$ $d=23.0$ Å): $\sigma_{total}=2.25$ Å and $\Gamma=0.575$.

Downloaded 27 Aug 2010 to 148.6.178.100. Redistribution subject to AIP license or copyright; see http://jap.aip.org/about/rights_and_permissions

sample 2, and sample 3 have comparable interfacial roughness, with σ values of 2.45, 2.4, and 2.25 Å, respectively. We note that the fits are better at higher angles. A larger σ would have fit the lower orders better but fit the higher orders much worse. Adding additional fitting parameters such as a larger surface roughness, a surface oxide layer, or an interfacial roughness that increases through the film can improve the fit. A choice of a non-Gaussian interfacial roughness could also be made to fit the data. However, we decided to fit with the simplest possible model realizing that it sets a lower limit on the interfacial roughness.

To obtain information on interfacial roughness correlation, we make offset-$(\omega,2\theta)$ scans and transverse (rocking) scans to probe the diffuse-intensity distribution. For all samples, the offset scans appear similar to the $(\omega,2\theta)$ scans, but with a much lower intensity. These results show that diffusely scattered x rays are concentrated in planes parallel to the surface centered around the multilayer Bragg conditions of each sample. In other words, diffuse x-rays scatter in phase at the multilayer Bragg conditions, evidence that at least a component of the interfacial roughness is vertically correlated through the film.

The procedure for fitting rocking curves has been described previously.[10] We treat the vertically correlated roughness as a structure factor modulating the intensity of the perfect multilayer stack. This treatment is justified because the diffuse intensity in the lateral vicinity of a Bragg reflection is dominated by that arising from the vertically correlated roughness. The structure factor is generated by considering the scattering from a single interface, e.g., a vacuum-surface interface. A rough surface can be characterized by specifying a height-height correlation function. We follow the approach of Sinha *et al.*,[28] by using a trial function, calculating the resultant transverse profile, and comparing with a measured curve. The form of the correlation function is chosen as

$$\langle Z(r-R)Z(r)\rangle=\sigma_{\mathrm{corr}}^2 \exp\left[-\left(\frac{|R|}{\xi}\right)^{2\alpha}\right], \qquad (1)$$

where $Z(r)$ is the displacement of the interface from its average position at location r, σ_{corr} is the rms roughness, ξ is the lateral correlation length, and α is a fraction between 0 and 1 that is related to the fractal dimension of the surface.[28] This form of correlation function treats the surface as rough (i.e., a self-affine fractal) on a short scale, but smooth on a large scale. Such a correlation function is said to have a long-wavelength cutoff. A consequence of the cutoff is a characteristic two-component transverse profile: an instrument limited peak in the specular direction and a clearly separable diffuse background. A profile from a surface that, on the other hand, had self-affine roughness for all length scales would appear as a single smoothly varying function peaked in the specular direction.

Figure 3 shows rocking (transverse) scans through the fifth-order Bragg peaks of samples 1 and 2 and through the third-order Bragg peak for sample 3 using $\lambda=1.54$ Å, along with fits to these data. The measurements consist of two-component profiles, a sharp central spike at the Bragg condition corresponding to the specular reflection and a broad peak arising from diffusely scattered x rays. The fit parameters are σ_{corr}, the rms amount of vertically correlated roughness, ξ, the lateral correlation length of the vertically correlated roughness, and α. All fits use $\alpha=1/2$. The results of the fitting are $\sigma_{\mathrm{corr}}=1.25\pm0.2$ Å and $\xi=60\pm20$ Å for sample 1, $\sigma_{\mathrm{corr}}=1.1\pm0.2$ Å and $\xi=80\pm20$ Å for sample 2, and $\sigma_{\mathrm{corr}}=0.8\pm0.2$ Å, and $\xi=100\pm20$ Å for sample 3. The magnitudes for correlated roughness derived from this analysis do not account for the total interfacial roughness. The remaining roughness can be accounted for by including a component that is randomly correlated vertically through the film. Such a component might arise from interdiffusion or nonaccumulating mistakes in replicating interfacial roughness. The magnitude of the uncorrelated component can be derived from[10]

$$\sigma_{\mathrm{random}}^2=\sigma_{\mathrm{total}}^2-\sigma_{\mathrm{corr}}^2. \qquad (2)$$

Another possibility is that while the roughness is well correlated vertically, the correlation is not perfect. Partially correlated roughness would contribute less diffuse intensity in the plane of the Bragg condition and our analysis would set a lower limit on its magnitude.

Transverse scans through the first-order Bragg peaks of samples 1, 2, and 3 using $\lambda=13.0$ Å, $\lambda=10.6$ Å, and $\lambda=13.5$ Å, respectively are shown in Fig. 4. The scans have the same general appearance as those for $\lambda=1.54$ Å, showing a central peak and a diffuse background. The main difference is that the diffuse component is relatively much weaker for these measurements than for those using $\lambda=1.54$ Å. The first diffraction order is attenuated much less by roughness than a higher order and consequently a smaller fraction of the specular-beam intensity is transferred into the diffuse background for a first order. Fits calculated using the specified values for λ are plotted as solid lines. The results of the fitting are $\sigma_{\mathrm{corr}}=1.0\pm0.2$ Å and $\xi=70\pm20$ Å, $\sigma_{\mathrm{corr}}=0.95\pm0.2$ Å and $\xi=90\pm20$ Å, and $\sigma_{\mathrm{corr}}=1.2\pm0.2$ Å and $\xi=100\pm20$ Å, values that are in basic agreement with the hard-x-ray results.

The depth probed by the different wavelengths can be estimated using values for the attenuation coefficients[29] of W and C. We use the depth at which reflected intensity is reduced to $1/e$ of its unattenuated value as a measure of the depth sampled. Interfaces below this depth contribute little to the reflectance. Interfaces located above this depth will contribute, with the top interfaces contributing most strongly. The value of the $1/e$ depth will depend on the diffraction conditions. For the soft-x-ray measurements at the first diffraction order, the $1/e$ depth is $\sim$200 Å for all the samples. For the Cu $K\alpha$ measurements through the fifth order for samples 1 and 2 and the third order for sample 3, this depth is greater than 3000 Å. The total thicknesses of sample 1 ($\sim$800 Å) and samples 2 and 3 ($\sim$1600 Å) are larger than the $1/e$ depth, 200 Å, for soft x-rays. Thus, with the soft x rays only interfaces in the upper 1/4 (1/8) of the film thickness for sample 1 (samples 2 and 3) are being probed. For the $\lambda=1.54$ Å measurements, the $1/e$ depth is greater than the sample thick-

Downloaded 27 Aug 2010 to 148.6.178.100. Redistribution subject to AIP license or copyright; see http://jap.aip.org/about/rights_and_permissions

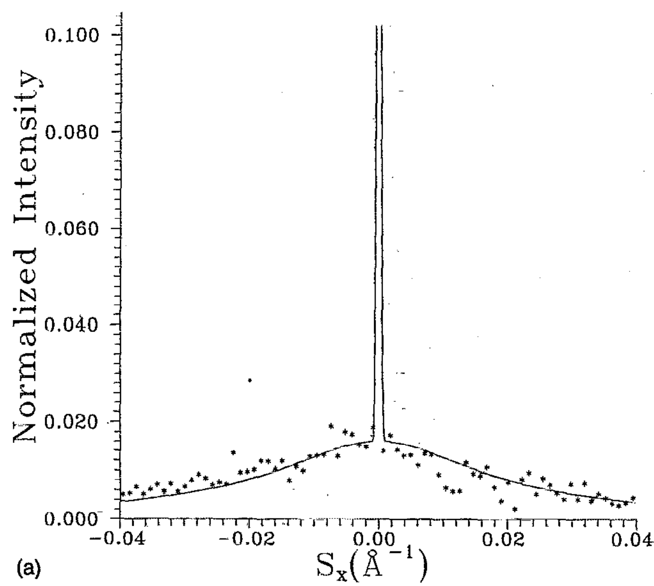

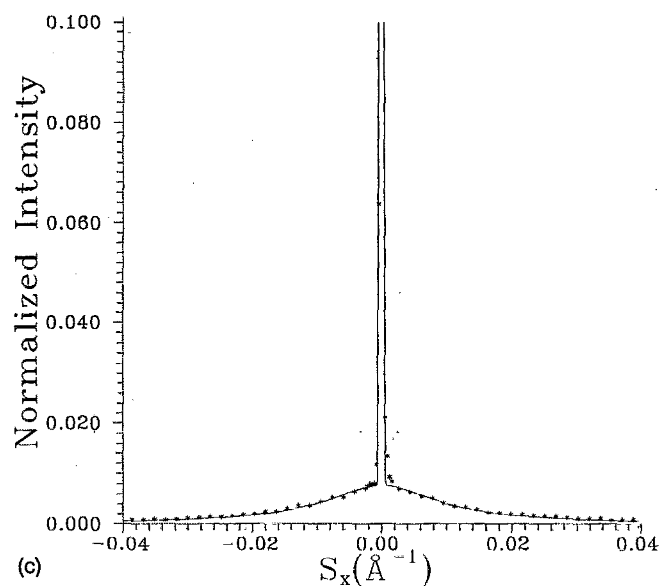

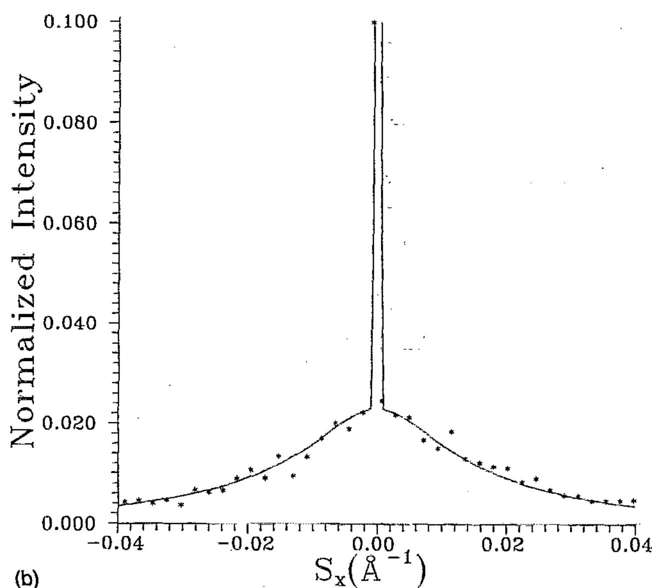

FIG. 3. Rocking (transverse) scans using $\lambda=1.54$ Å. The solid curves are theoretical fits. (a) Sample 1 ($n=20$ $d=36.7$ Å): scan through the fifth-order ($2\theta=12.04°$) Bragg peak. Fit parameters are $\sigma_{\text{corr}}=1.25$ Å, $\xi=60$ Å, and $\alpha=1/2$. (b) Sample 2 ($N=55$ $d=30.46$ Å): scan through the fifth-order Bragg peak ($2\theta=14.56°$); $\sigma_{\text{corr}}=1.1$ Å, $\xi=80$ Å, and $\alpha=1/2$. (c) Sample 3 ($N=70$ $d=23.0$ Å): scan through the third-order Bragg peak ($2\theta=11.55°$); $\sigma_{\text{corr}}=0.8$ Å, $\xi=100$ Å, and $\alpha=1/2$. The data are plotted on linear scales magnified so that the details of the diffuse component are emphasized. The peak intensities are normalized to one.

ness and all interfaces contribute significantly to the reflected intensity. The independence of wavelength, in the measurements, of the interfacial roughness values is strong evidence that the interfacial roughness is not changing through the film.

The results of our x-ray characterization explain why such films perform well in soft x-ray imaging applications. First, the small magnitude of the total interfacial roughness keeps the attenuation of the specular reflection low, even for short-period multilayers. Second, although vertically correlated roughness makes a significant contribution to the total roughness, it occurs primarily for short wavelengths (as shown by the small values of the lateral correlation length). Consequently, diffuse intensity is scattered at relatively large angles and so will be excluded by apertures in optical systems. The absence of long-wavelength correlated roughness arises because interfaces are smooth at these length scales. The power spectrum, the Fourier transform of the height-height correlation function, can be used to make quantitative statements about the scattering strength in various wavelength ranges. For an exponential correlation function, the power spectrum is a Lorentzian with a full width at half-maximum that depends on ξ. Using $\xi=10$ nm, a typical value for sputter deposited W/C, we integrate the power spectrum over various frequency ranges. Converting frequency to wavelength, we find that 90% of the mean square roughness due to vertically correlated roughness arises from wavelengths in the 10–1000 nm range. We have no information about the power spectrum of the random component. However, it is only the diffuse scattering arising from the correlated roughness that contributes significant intensity in the vicinity of the specular reflection at the Bragg conditions.

It is always possible that roughness exists on lateral scales much larger than can be resolved by the instrument. However, because we observe a two-component transverse profile, the roughness must cut off (or at least be greatly reduced) at long wavelengths, i.e., in the range of 1000 nm

Downloaded 27 Aug 2010 to 148.6.178.100. Redistribution subject to AIP license or copyright; see http://jap.aip.org/about/rights_and_permissions

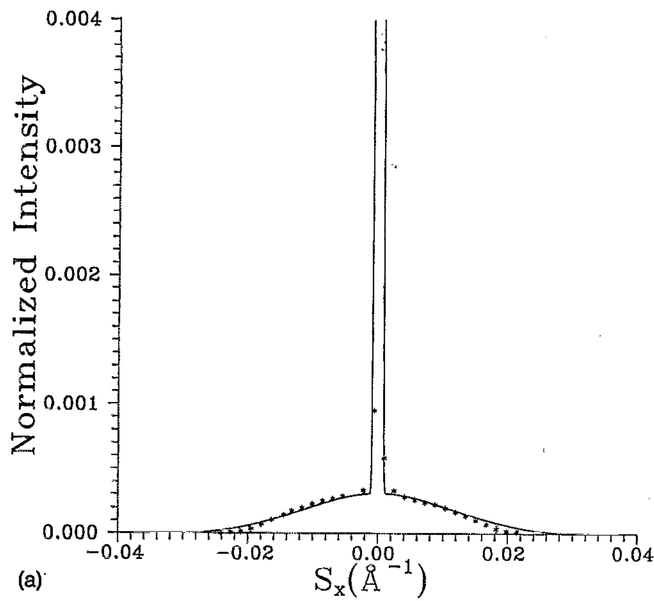

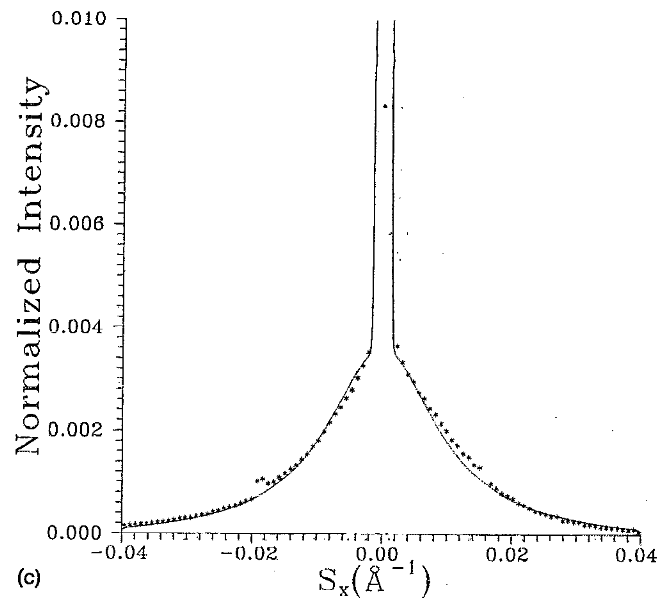

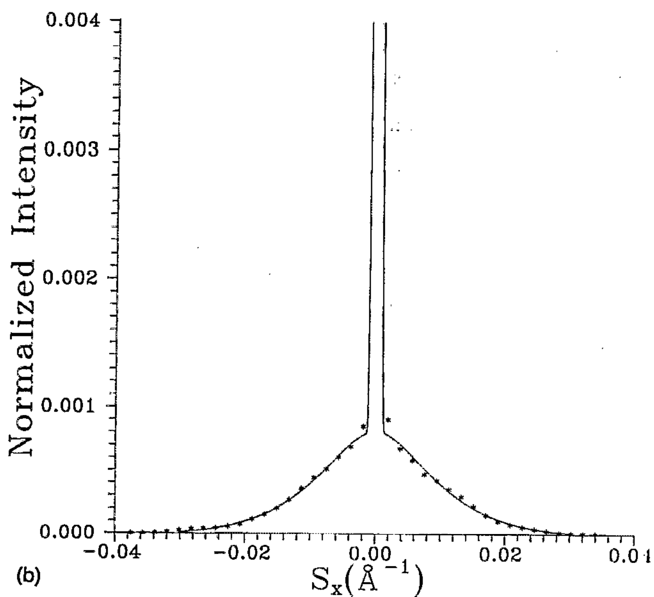

FIG. 4. Rocking (transverse) scans through the first-order Bragg peak using soft x rays. The solid curves are theoretical fits. (a) Sample 1 ($n=20$ $d=36.7$ Å): scan with $\lambda=13.0$ Å, $2\theta=20.4°$; $\sigma_{\text{corr}}=1.0$ Å, $\xi=70$ Å, and $\alpha=1/2$. (b) Sample 2 ($N=55$ $d=30.46$ Å): scan with $\lambda=10.6$ Å, $2\theta=14.56°$; $\sigma_{\text{corr}}=0.95$ Å, $\xi=90$ Å, and $\alpha=1/2$. (c) Sample 3 ($N=70$ $d=23.0$ Å): scan with $\lambda=13.47$ Å, $2\theta=33.98°$; $\sigma_{\text{corr}}=1.2$ Å, $\xi=100$ Å, and $\alpha=1/2$.

and beyond. It is unlikely that any such large-scale roughness would arise as a result of the growth process. For the experimental conditions reported here, features with size or separation on the scale of 2.0 μm should be resolvable. This number is arrived at from the width of the central peak measured with Cu $K\alpha$.

In summary, we have characterized interfacial roughness of W/C multilayers using $\lambda=1.54$ Å, and λ in the range of 10–13 Å. We extract quantitative values for the amount and lateral correlation length of the vertically correlated roughness and find that the values are relatively independent of the wavelength. This is interpreted to mean that interfacial roughness is changing very little or not at all with depth into the film. It is of course, very likely that the outermost interface is considerably rougher than internal interfaces, because of the possibility of oxidation or corrosion. It is dangerous to draw conclusions[23] on average interfacial roughness from outer-surface roughness. Finally, we conclude that characterization of the performance of soft x-ray optical elements can be performed using hard x-rays for films where the interfacial roughness does not change through the film. However, there is no *a priori* way of knowing whether roughness changes. Characterization with soft x rays in the range of desired operation of the optical elements and comparison with hard x-ray measurements can provide a direct answer. The multilayer films reported on here, because roughness is not varying with depth, can be useful for all energy ranges without correction for changing mean roughness. This fortunate circumstance is likely not to be general, as the possible buildup of roughness depends on a number of kinetic parameters in film growth. Through comparisons such as the ones described here, it should be possible to establish for a variety of materials combinations and process parameters that define when a sample roughens and when it does not.

Downloaded 27 Aug 2010 to 148.6.178.100. Redistribution subject to AIP license or copyright; see http://jap.aip.org/about/rights_and_permissions

ACKNOWLEDGMENTS

This work was supported by NSF Grant No. DMR92-01856. J. M. is supported by NIH Grant No. CH5247. The soft x-ray research was conducted at the Synchrotron Radiation Center, University of Wisconsin, which is supported by NSF Grant No. DMR92-12658.

[1] A. M. Hawryluk and L. G. Seppala, J. Vac. Sci. Technol. B **6**, 2162 (1988).

[2] I. Lovas, W. Santy, E. Spiller, R. Tibbetts, and J. Wilczynski, Proc. SPIE **316**, 90 (1981).

[3] D. L. Shealy, R. B. Hoover, T. R. Barbee, and A. B. C. Walker, Opt. Eng. **29**, 721 (1990).

[4] G. Margaritondo and F. Cerrina, Nucl. Instrum. Methods A **291**, 26 (1990).

[5] A. B. C. Walker, T. R. Barbee, R. B. Hoover, and J. F. Lindblom, Science **241**, 1781 (1988).

[6] L. Golub, M. Herant, K. Kalata, I. Lovas, G. Nystrom, E. Spiller, and J. Wilczynski, Nature **344**, 842 (1990).

[7] For optical multilayers, see J. M. Eastman, in *Physics of Thin Films*, edited by G. Hass and M. H. Francombe (Academic, New York, 1978), Vol. 10, pp. 167–226.

[8] E. Spiller and A. E. Rosenbluth, Opt. Eng. **25**, 954 (1986).

[9] J. E. Harvey, W. P. Zmek, and E. C. Moran, Proc. SPIE **1160**, 209 (1989).

[10] D. E. Savage, J. Kleiner, N. Schimke, Y.-H. Phang, T. Jankowski, J. Jacobs, R. Kariotis, and M. G. Lagally, J. Appl. Phys. **69**, 1411 (1991); D. E. Savage, N. Schimke, Y.-H. Phang, and M. G. Lagally, *ibid.* **71**, 3283 (1992).

[11] J. B. Kortright, J. Appl. Phys. **70**, 3620 (1991); J. B. Kortright, T. D. Nguyen, I. M. Tidswell, and C. A. Lucas, in *Physics of Multilayer Structures* (Optical Society of America, Washington D. C., 1992) p. 102.

[12] J. M. Slaughter and C. M. Falco, Proc. SPIE **1742**, 365 (1992).

[13] B. M. Clemens, A. P. Payne, and S. Brennan, Opt. Soc. Am. Tech. Digest Ser. **7**, 105 (1992).

[14] A. Bruson, C. Dufour, B. George, M. Vergnat, G. Marchal, and Ph. Mangin, Solid State Commun. **71**, 1045 (1989).

[15] S. K. Sinha, Physica B **173**, 25 (1991).

[16] Y. -H. Phang, D. E. Savage, T. F. Keuch, M. G. Lagally, J. S. Park, and K. L. Wang, Appl. Phys. Lett. **60**, 2986 (1992).

[17] S. Nayak, J. M. Redwing, T. F. Kuech, Y.-H. Phang, D. E. Savage, and M. G. Lagally, Mater. Res. Soc. Symp. Proc. (in press).

[18] Z. H. Ming, A. Krol, Y. L. Soo, Y. H. Kao, J. S. Park, and K. L. Wang, Phys. Rev. B **47**, 16 373 (1993).

[19] D. G. Stearns, J. Appl. Phys. **71**, 4286 (1992).

[20] Y.-H. Phang, R. Kariotis, D. E. Savage, and M. G. Lagally, J. Appl. Phys. **72**, 4627 (1992).

[21] S. K. Sinha, M. K. Sanyal, S. K. Satija, C. F. Majkrzak, I. K. Schuller, H. Homma, C. M. Falco, and B. N. Engel, Opt. Soc. Am. Tech. Digest Ser. **7**, 82 (1992).

[22] Y.-H. Phang, D. E. Savage, R. Kariotis, and M. G. Lagally, J. Appl. Phys. **74**, 3181 (1993).

[23] E. Spiller, J. Wilczynski, D. Stearns, L. Golub, and G. Nystrom, Appl. Phys. Lett. **61**, 1481 (1992).

[24] E. E. Fullerton, I. K. Schuller, and Bruynseraede, Mater. Res. Soc. Bull. **17**, 33 (1992).

[25] J. F. MacKay, D. W. Pearson, P. M. DeLuca, M. N. Gould, and M. G. Lagally (unpublished).

[26] See for example B. L. Henke, J. Y. Uejio, H. T. Yamada, and R. E. Tackaberry, Opt. Eng. **25**, 937 (1986).

[27] B. G. Peterson, L. V. Knight, and H. K. Pew, Proc. SPIE **563**, 328 (1985).

[28] S. K. Sinha, E. B. Sirota, S. Garoff, and H. B. Stanley, Phys. Rev. B **38**, 2297 (1988).

[29] B. L. Henke, J. C. Davis, E. M. Gullikson, and R. C. C. Perera, Report No. LBL-26259, UC-411, November 1988.

Downloaded 27 Aug 2010 to 148.6.178.100. Redistribution subject to AIP license or copyright; see http://jap.aip.org/about/rights_and_permissions